Support information

Increasing the Oxygen-Containing Functional Groups of Oxidized Multi-Walled Carbon Nanotubes to Improve High-Rate-Partial-State-of-Charge Performance

Characterization of the materials

X-ray diffraction (XRD) measurements of the as-prepared materials were conducted using a Rigaku Ultima IV diffractometer with Cu Ka radiation (l ¼ 0.1548 nm) in steps of 0.02, the relative contents of substances in different samples were calculated by using the strongest peak. transmission electron microscopy (FEI Tecnai F30, 300 kV) were employed to observe effect of acid pickling on multi walled carbon nanotubes.

Study on hydrophilicity of MWCNTs suspension

By taking a quantitative solution in 9 $mg \cdot ml^{-1}$ multi walled carbon nanotubes, pour them into the glass bottle as shown in Fig. S3, shake the glass bottle fully, after standing for one hour, the state of multi wall carbon nanotube suspension was observed.

Schematic diagram of oxygen-containing functional groups on multi wall carbon nanotubes

The change trend of different kinds of oxygen-containing groups was indicated by the

length of acid-treatment time，As shown in the Fig. S4.

Specific numerical table of electrochemical performance of lead-acid battery

In this experiment, the energy storage performance of the battery is mainly characterized by electrochemical test, including EIS CV capacity and cycle life. EIS of negative plate is used for equivalent circuit fitting of impedance data, as shown in the Fig.4A. The classical R (Q (RZ)) equivalent circuit is used, and the fitting results are shown in table.S1. Where R_S corresponds to the ohmic resistance of electrolyte, Rct is the charge transfer resistance in electrochemical process, Z_W is the Warburg impedance, which is related to diffusion.

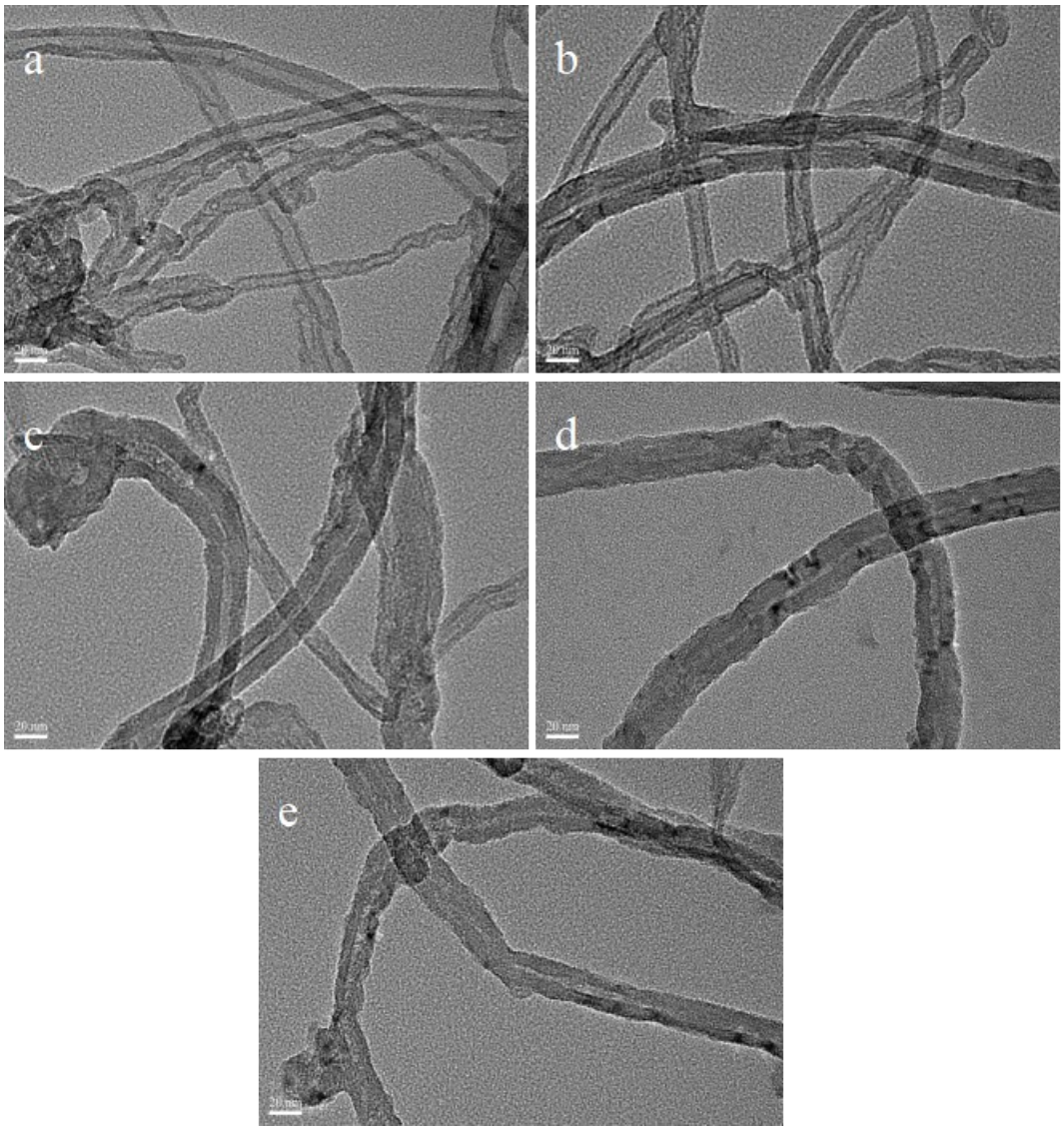

Fig. S1. TEM images of different carbon samples: MWCNTs (a), MWCNTs-2h (b), MWCNTs-6h (c), MWCNTs-12h (d) and MWCNTs-24h (e).

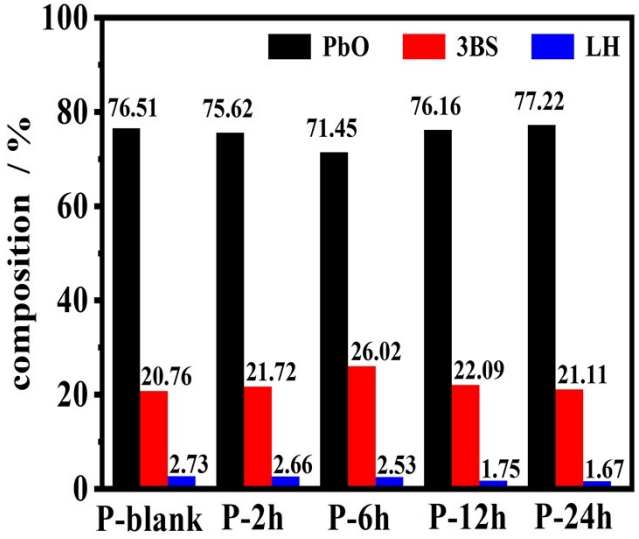

Fig. S2. Compositions of the NAMs collected from the interior of the cured negative plates.

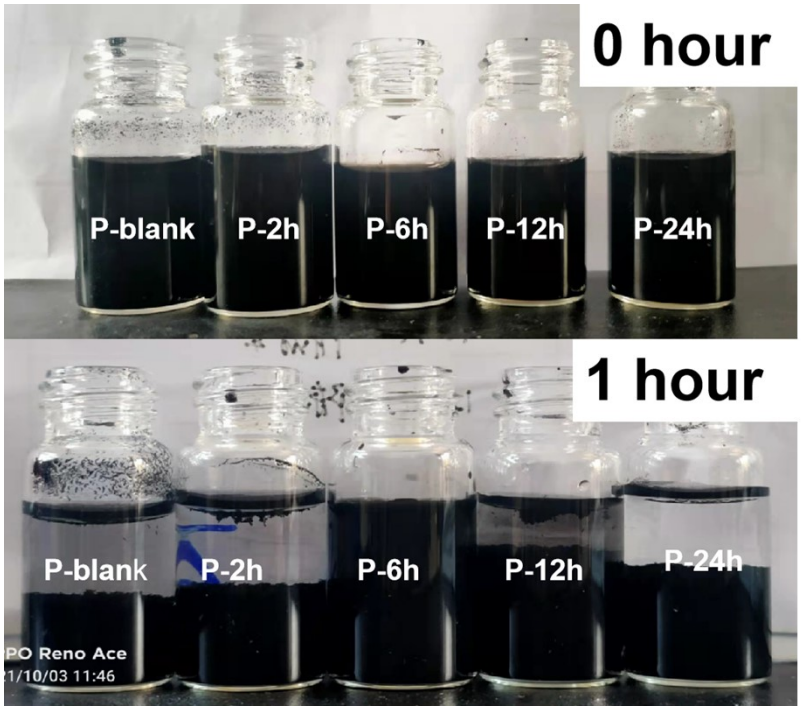

Fig. S3. Physical diagram of hydrophilicity of multi wall carbon nanotubes

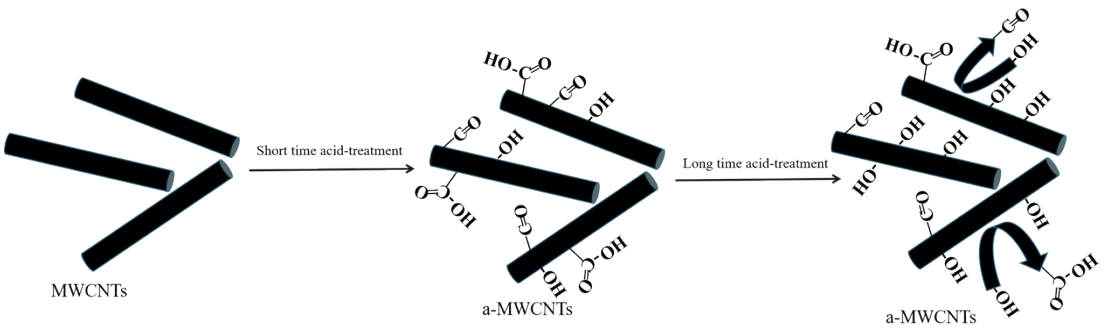

Fig. S4. Schematic diagram of oxygen-containing functional groups on multi wall carbon nanotubes

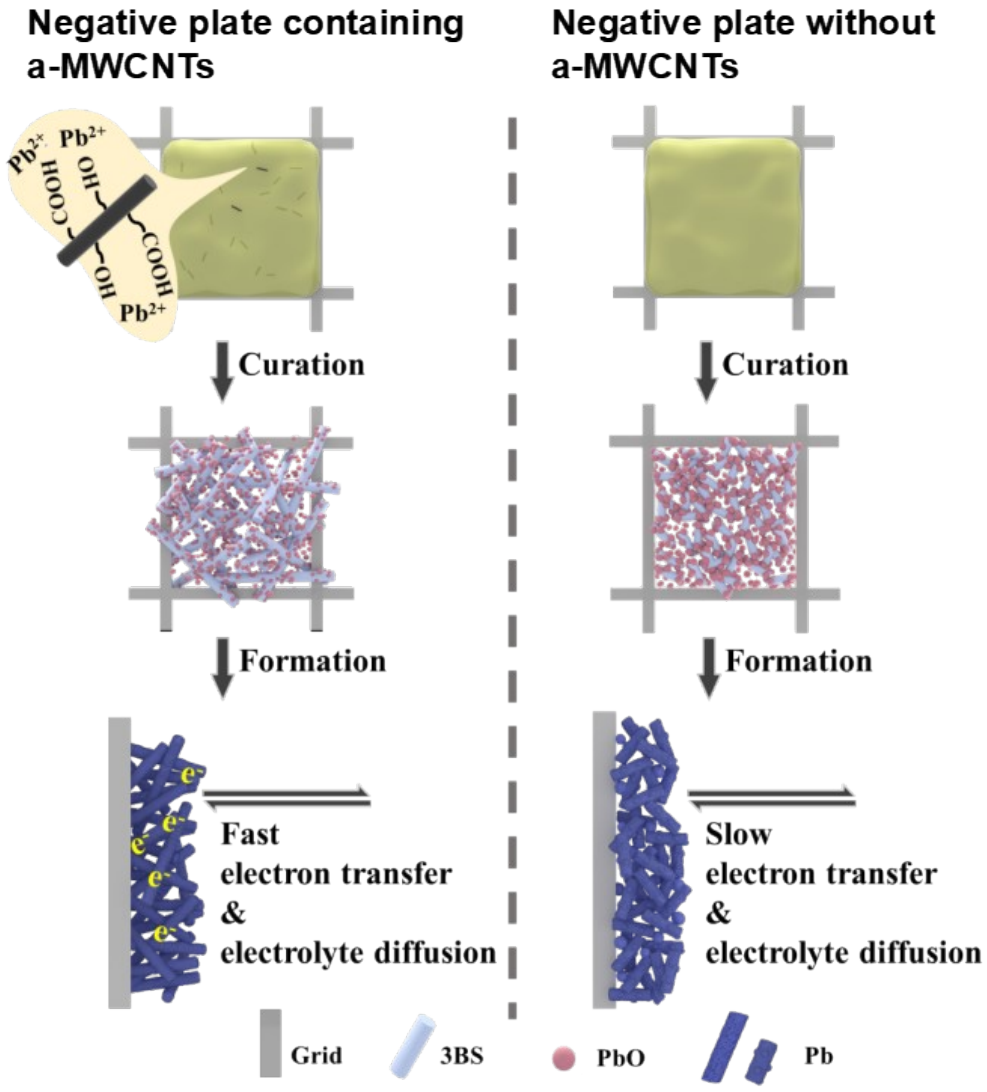

Fig. S5. Schematic diagram of HRPSoC enhancement mechanism of battery assembled with negative plate containing a-MWCNTs

Table. S1 Simulation in equivalent circuits of the EIS spectra of different plates

Samples	R_s ($\Omega \cdot cm^2$)	*Electroconductivity* ($S \cdot cm^{-2}$)	Q_{dl} ($Ss^n \cdot cm^{-2}$)	R_{ct} ($\Omega \cdot cm^2$)	Z_W ($Ss^n \cdot cm^{-2}$)	Error (%)
P-blank	0.09126	47.53	0.976	0.1026	136.8	1.2386
P-2h	0.072037	47.55	1.141	0.0937	125.7	0.8756
P-6h	0.05739	47.94	1.225	0.0701	76.4	0.8796
P-12h	0.06086	49.15	1.158	0.0875	88.1	1. 3588
P-24h	0.07047	49.15	0.977	0.0984	130.7	1. 7585

Table. S2 Specific values of capacitance and number of cycles

Electrochemical properties	Plate-blank	Plate-2h	Plate-6h	Plate-12h	Plate-24h
Capacity/mAh	0.6257	0.7687	0.8176	0.7838	0.7384
Cycle number	19712	26430	39580	33764	21915

Table. S3 Specific values associated with CV tests

Samples	Oxidation peak current	Reduction peak current	Oxidation peak area	Reduction peak area	Oxidation potential	Reduction potential
P-blank	1.863	-1.716	0.618	0.452	-0.708	-1.863
P-2h	2.717	-2.400	0.755	0.615	-0.849	-1.225
P-6h	3.504	-3.036	0.912	0.767	-0.576	-1.218
P-12h	2.950	-2.789	0.925	0.740	-0.832	-1.250
P-24h	2.329	-1.971	0.739	0.478	-0.786	-1.259